

# Site characterization through the use of Computational Fluid Dynamics

Konstantinos Vogiatzis<sup>a</sup>, David S. De Young<sup>b</sup>

<sup>a</sup>AURA New Initiatives Office; Tucson, AZ 85719, USA

<sup>b</sup>NOAO; Tucson, AZ 85719, USA

## ABSTRACT

Numerical simulations of airflow over various potential sites for extremely large telescopes have been performed. Information such as wind speed, turbulence levels (fluctuating velocity RMS), wake lengths, boundary (ground) layer thickness and the effects of topographically induced turbulence on “seeing” can be retrieved, thus providing an essential evaluation tool in the site selection process. We present a sample set of simulations carried out over possible site locations for a 20-30m-telescope project. Simulations at several different sites located in Chile were performed in terms of wind speed levels and the effects of the local topographic features on the flow in the summit region, namely turbulent intensity and boundary layer thickness, under the prevailing wind conditions. Results indicate that the turbulent boundary layer thickness, defined as the region of considerable turbulent intensity levels, ranges from 10m to ~400m, depending on peak location and wind direction, for summit wind speeds varying between 4 and 12 m/s.

**Keywords:** Site characterization, CFD, Wind flow, Turbulence, Digital Elevation Maps

## 1. INTRODUCTION AND MOTIVATION

Atmospheric turbulence is one of the main causes of image degradation in optical astronomy. It covers a wide range of spatial and temporal scales and can be induced by local topography or by high altitude shear (jet-stream). A variety of instruments have been and are still being developed and tested for site characterization through turbulence induced seeing measurements, but the effect of ground layer is not yet well understood.

Computational Fluid Dynamics (CFD) can be considered as a complementary tool to site quality campaigns. This technique provides detailed airflow information over an arbitrarily chosen variety of initial and boundary conditions in the applicable Reynolds number ranges, and the calculations can be performed relatively quickly and at minimal cost. One of the earliest applications of CFD to site characterization involved ground layer turbulence investigation above the Gemini sites on Mauna Kea, HI, and Cerro Pachon, Chile (De Young & Charles 1995). The advances in computational power permitted in recent years a more widespread and elaborate use of CFD but on the meso-scale level (Riemer & Zängl 2002).

In this paper we provide an overview of results of CFD modeling of wind flow above candidate very large telescope sites, with the emphasis here on topographically induced turbulence. The motivation for this study is threefold. The first objective is to provide an overview of the kinds of analysis tools that NOAO is developing and making available to the community of groups that are engaged in site characterization and selection procedures for very large telescopes. The second goal is to provide a set of results of wind flow modeling above existing telescope sites, for which wind and seeing measurements are planned or are already available. Comparison of such data with results from calculations can be essential in verifying the numerical method and for future planning of site quality tests. The final goal is to investigate the behavior of wind flow above various types of sites such as a high altitude inland site or a coastal site and gain insight into possible peculiarities they may exhibit.

## 2. METHOD OF CALCULATION

The calculations were fully three-dimensional, and the flow was assumed to be incompressible and isothermal. The effects of turbulence were modeled through the use of the  $k-\epsilon$  approximation, modified to account for high Reynolds number effects, and commercial software (STAR-CD) was used to solve the Navier-Stokes equations. In principle, species concentration and conjugate heat transfer/radiation effects can be incorporated into the calculations, but these are not included in the results shown here.

## 2.1 Computational domain, Initial and Boundary Conditions

The first step in performing numerical simulations is always grid generation. The terrain has to be modeled as part of the grid boundary. Although the software in use is capable of solving in arbitrary grids, performance can be improved if a uniform grid is used in both horizontal directions. Topographic data of non-US sites are not readily available in a uniform rectilinear form so additional commercial software and in-house developed code had to be used to convert the data. Scanned contour topographic maps in CAD file format were translated to ASCII triads (X, Y, Z) with fixed horizontal spatial resolution, which became the rectangular basis of the grid. The X and Y values are UTM coordinates (m) while Z is the elevation (m). Such a file is known as Digital Elevation Model or Map (DEM). To generate the third dimension of the grid a given number of points were placed between the local surface elevation and the chosen (fixed) ceiling elevation. The vertical distance between two consecutive nodes was chosen to be a term of a geometric series with ratio of 1.2. As a result, a vertical spatial resolution of approximately 1m was achieved close to the ground, where high velocity gradients exist. Close to the ceiling, where the airflow is expected to be more uniform, the resolution can be as coarse as 400m. The vertical resolution of a representative grid is shown in Figure 1.

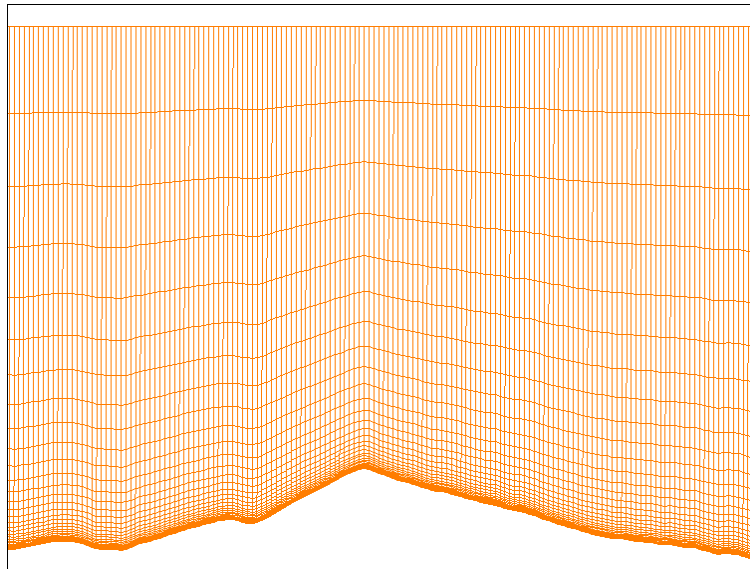


Figure 1. Vertical cross-section of a representative grid.

For improved accuracy the resulting computational box orientation was chosen so that a face was always normal to the applied wind direction. The inlet wind velocity profile is generally given by  $u(z) = U[(z - z_0)/h]^{0.6}$ . The value of  $z_0$  was dictated by the local surface elevation at the inlet, while  $U$  and  $h$  were chosen to yield a wind speed of  $15 \text{ m sec}^{-1}$  at 6000m, a reasonable value for Chile. It is important to note that this profile is more realistic than a uniform wind speed level and also more correct than the traditional 1/7 power law for flat plate turbulent boundary layer. Atmospheric boundary layer measurements (Davenport 1960) indicated that over rough terrain the exponent for a stable layer, such as a nocturnal one, could be as high as 0.6, rather than 0.15-0.2, which is often recorded during the day. The inlet air properties were taken to be those of the atmosphere at the average elevation of the computational domain. The inlet air was given a turbulent intensity of 5%, that is the rms value of the fluctuating part of the velocity was 5% of the local (free stream) velocity value. The other parameter of the turbulence model, the rate of turbulent energy dissipation, was calculated from the turbulent kinetic energy, by assuming a mixing length of 5m and equilibrium between turbulent energy production and dissipation. On the topographic surface a no slip boundary condition was placed with a roughness height of 0.01m, a good approximation for arid Chilean sites (Wieringa 1996). The sides and ceiling of the domain were given free slip boundaries with a zero normal velocity component; the outflow boundary condition set all normal derivatives to zero.

### 2.1.1 Las Campanas

As a first validation task, flow over an existing telescope site was undertaken. In particular, flow over the summit of Manqui, Las Campanas, the Magellan site, was considered under the two prevailing wind directions,  $45^\circ$  (NE) and  $225^\circ$

(SW) azimuth (private com. 2003). The DEM used in these calculations, along with the horizontal sub-domain, is shown in Figure 2. Its horizontal resolution is 20m, with a size of 22x24km and is centered at (335000,6788000) UTM. The sub-domain used in the calculations had a size of 10x8km, 40m horizontal resolution, a ceiling elevation of 6000m, 33 nodes in the vertical direction, and 1.6 million cells.

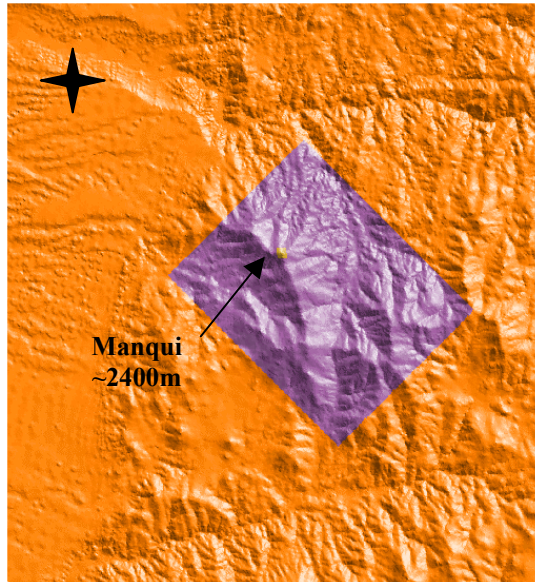


Figure 2. Digital Elevation Model of Las Campanas region.

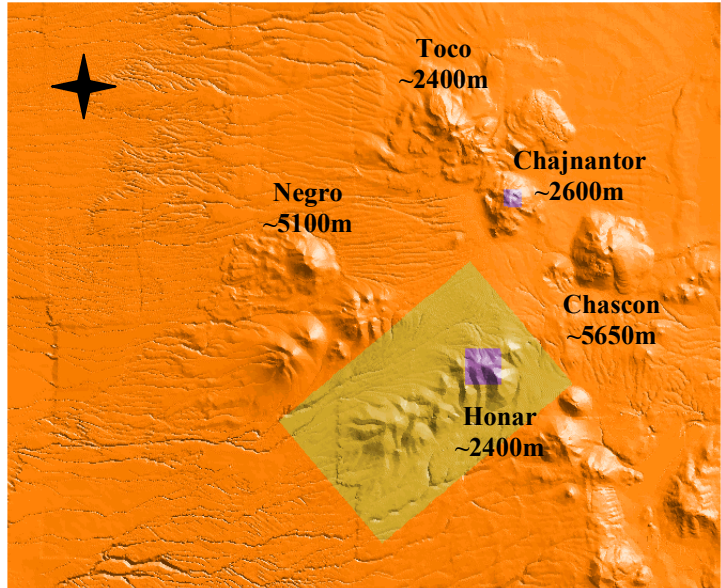


Figure 3. Digital Elevation Model of the Atacama plateau.

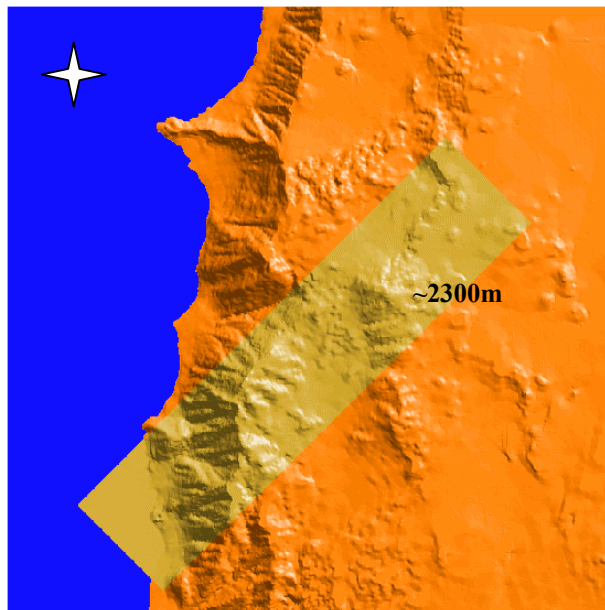


Figure 4. Digital Elevation Model of a coastal site

### 2.1.2 Atacama plateau

A processed DEM 40x33km in size was used as the basis for the calculations presented here and can be seen in Figure 3. The horizontal resolution of this DEM is 10m and its center UTM coordinates are (621000,7452500). To determine the effects of large-scale topographic features on the airflow over the plateau, to identify peaks of interest or concern, and to obtain a first estimate of turbulent boundary layer thickness, a coarse resolution calculation over a wide region was

required. We considered therefore the flow over the whole plateau with a domain size 24x30km, 240m horizontal resolution, 33 vertical nodes, resulting in 400,000 cells. Wind from the west was used in this case, since this is the prevailing wind direction in the region (Sakamoto et al 2000). The next objective was to examine the behavior of the boundary layer and to quantify its intensity close to a summit of interest. Higher resolution calculations were in need then: flow over Cerros de Honar, domain size 2x2km, 20m horizontal resolution, 31 vertical nodes, resulting in 300,000 cells, and flow over Cerro Chajnantor, domain size 1x1km, 10m horizontal resolution, with the same number of vertical nodes and total cells. In these two cases we used as inlet conditions the output from the first coarse resolution calculation. Finally, flow over Cerros de Honar under a different wind direction, that of 230° azimuth (SW), was also considered for reasons that will be discussed in section 3. In this case we used a domain size of 9x14km, 200m horizontal resolution, 33 vertical nodes, resulting in 100,800 cells. The ceiling for the above calculations was set at 8000m. The three sub-domains are also marked in Figure 3.

### 2.1.3 South American coastal site

The object of this test was to compare the airflow behavior over a given coastal site under two different wind directions, one from the mainland over relatively smooth terrain and one from the sea, over a steep rise. A processed 40m horizontal resolution DEM 22x24km in size was used in this case and can be seen in Figure 4. The first calculation used NE wind (45°), a 5x8km domain, 200m horizontal resolution, 34 vertical nodes, resulting in 33,000 cells. The second calculation, which included the coastline, used SW wind (225°), a 5x18km domain, same horizontal resolution and vertical nodes, resulting in 74,250 cells. Both computational domains were given a ceiling of 6000m. The two sub-domains are also shown in Figure 4.

## 3. RESULTS

### 3.1 Las Campanas

Sample graphs for airflow above the summit of Manqui are shown in Figures 5 and 6 for both wind directions. All plots are made in the vertical plane that passes through the peak and runs along the NE-SW axis of the domain (parallel to wind direction). Figure 5 presents velocity magnitude contours for the NE wind case and, as can be clearly seen, the wind speed in a 50m layer above the summit is between 7.5 and 8.5 m sec<sup>-1</sup>, value in good agreement with measurements, as reported to the authors (private com. 2003). Figure 6 shows the turbulent rms velocity contours for both NE and SW wind flow directions. The calculated boundary layer thickness is marked in each graph. The cutoff height is taken to be that, after which turbulence intensity drops to the input free-stream level (~5%). As expected the NE case exhibits a thicker boundary layer (50m against 25m for the SW case) due to the rougher terrain to the NE of the site, as one can observe in Figure 2. The slopes of Manqui are such, however, that the summit's wake in the SW case is more turbulent.

### 3.2 Atacama plateau

An effective way of identifying potential problems on candidate sites due to wakes caused by neighboring mountainous masses is examining the turbulence levels on horizontal cuts at various elevations. For instance, Figure 7 shows turbulent rms velocity contours above the plateau at two different elevations, 5000m and 5400m. The complex structure of the wake produced by the base of the Toco-Chajnantor-Honar axis is visible in the left image, as well as the fact that all the peaks to the west of that axis lie in low turbulence stream. From the right graph one can assume that none of the high peaks (Toco, Chajnantor, Chascon, Honar) is inside a wake when the wind is from the west, but under different wind directions they may cause problems for each other or for the lower peaks of the plateau, since they produce wakes that reach or exceed 10km in length.

To ascertain whether a mountain's own slopes can cause problems on the summit one must examine the higher resolution small-scale results of rms velocity contours. As an example Figure 8 (left) shows the behavior of the boundary layer on top of Honar. Under west winds the layer is rather benign with a thickness of 45m (defined as before) over a smooth slope. However, if the wind shifts to the SW, as shown in the right graph, the thickness jumps to 200m due to the fact that the flow passes above the whole ridge (as can also be seen in Figure 3), which exhibits a large-scale saw-tooth profile. As another example, in Figure 9 we present the turbulent rms velocity contours on the summit of Chajnantor. Although unaffected by other volcanoes due to its high elevation, its own steep, rough western slope and rugged summit causes early separation resulting in a 120m medium-intensity boundary layer above the summit.

### 3.3 South American coastal site

Finally, Figure 10 presents velocity rms contours in vertical planes that pass through the summit aligned with the flow directions for the two examined coastal site cases. A very thin boundary layer is observed in the left image, when the wind blows over the smooth terrain to the NE. In contrast, the right graph reveals a thicker boundary layer, a result of the separation occurring as the flow clears the southwestern cliffs. However, turbulence intensity is low inside the layer and that may have minimal impact on seeing.

## 4. CONCLUSIONS

The brief overview of results presented here provides only a sample of the capabilities available through CFD simulations of wind flow above candidate sites for very large telescopes. Such calculations can provide mean and rms velocity fields, as well as vorticity, to calculate the intensity and measure the thickness of boundary layers and the length of wakes. They can also produce temperature fields and density gradients to characterize the thermal boundary layer of a potential site. The combined effect of mechanical and thermal turbulence is one of the key criteria in a site characterization procedure and CFD can help towards an optimum selection.

The next steps in site simulations include enhancements to spatial resolution as well as the inclusion of thermal effects, once information on temperature profiles upwind of the sites of interest becomes available. A post-processor has already been developed that relates mechanical and thermal turbulence output to Full Width Half Maximum values of the seeing disk along a given path. Thus the quality of a site can be more directly assessed. Further verification of the CFD results is also needed, and this can be achieved through additional wind and seeing measurements at existing telescope locations. As this work progresses, it is our intent to make both the tools and the results available to the entire very large telescope community, so that the overall progress in this rapidly emerging field can be enhanced.

## ACKNOWLEDGMENTS

The authors gratefully acknowledge the contribution of Rick Robles, NIO, who assisted with data translation, Alistair Walker, CTIO, Matt Johns, OCIW, and Mark Phillips, LCO, who provided digital topographic maps and participated in useful discussions.

## REFERENCES

1. D. S. De Young and R. D. Charles, "Numerical simulation of airflow over potential telescope sites", *Astron. J.* **110** (6), pp. 3107-3114, 1995.
2. M. Riemer and G. Zängl, *Analysis of the performance of the MM5 for the VLT site at Paranal*, Final Report ESO contract 66987/ODG/02/6685/GWI/LET, p. 163, Meteorologisches Institut der Universität München, München, 2002.
3. A. G. Davenport, "Rationale for determining design wind velocities", *Proc. ASCE J. Struct. Div.* **86**, pp. 39-68, 1960.
4. J. Wieringa, "Updating the Davenport roughness classification", *J. Wind Eng. & Ind. Aerodyn.* **65**, pp. 1-12, 1996.
5. M. Johns, OCIW, and M. Phillips, LCO, private communication, 2003.
6. S. Sakamoto, K. Handa, K. Kohno, N. Nakai, A. Otarola, S. J. E. Radford, B. Butler, and L. Bronfman, "Comparison of meteorological data at the Pampa La Bola and Llano de Chajnantor sites", NRAO/ALMA Memo 322, p. 19, 2000.

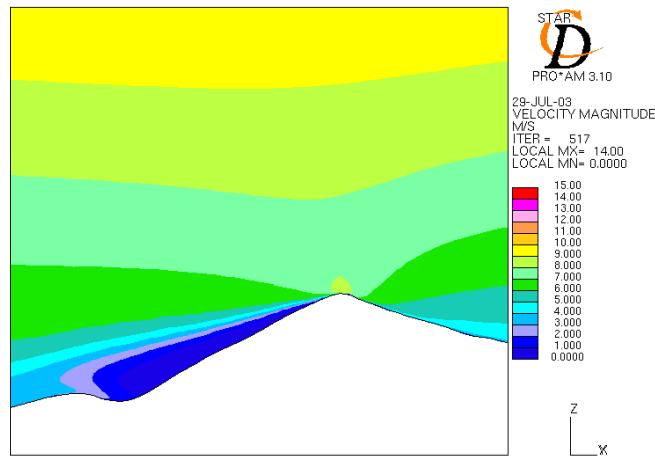


Figure 5. Manqui summit. Velocity contours in a vertical plane passing through the peak, aligned with the wind direction, NE. Resolution is 40m.

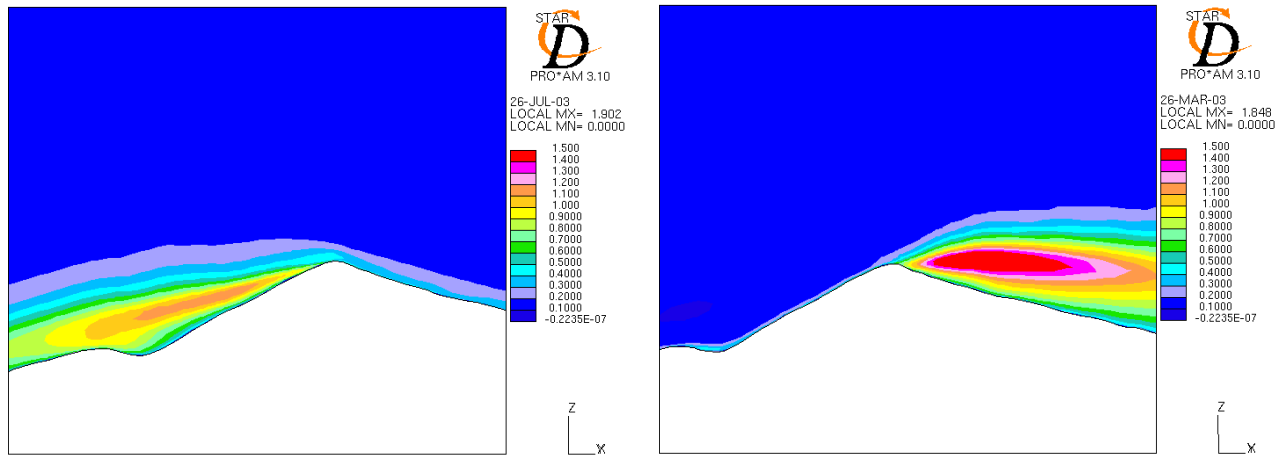


Figure 6. Manqui summit. Turbulent rms velocity contours, same plane and resolution as in Figure 4, for NE (left) and SW (right) wind directions.

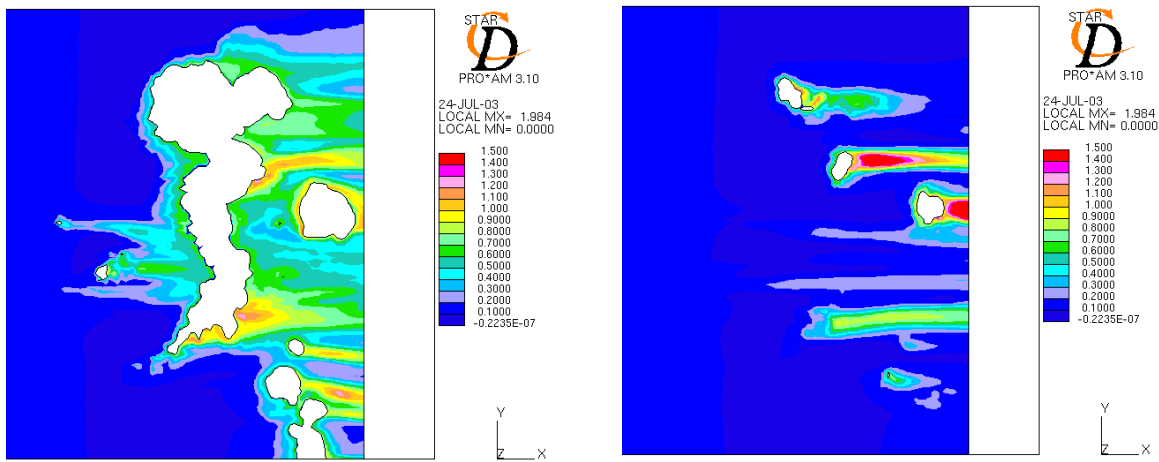
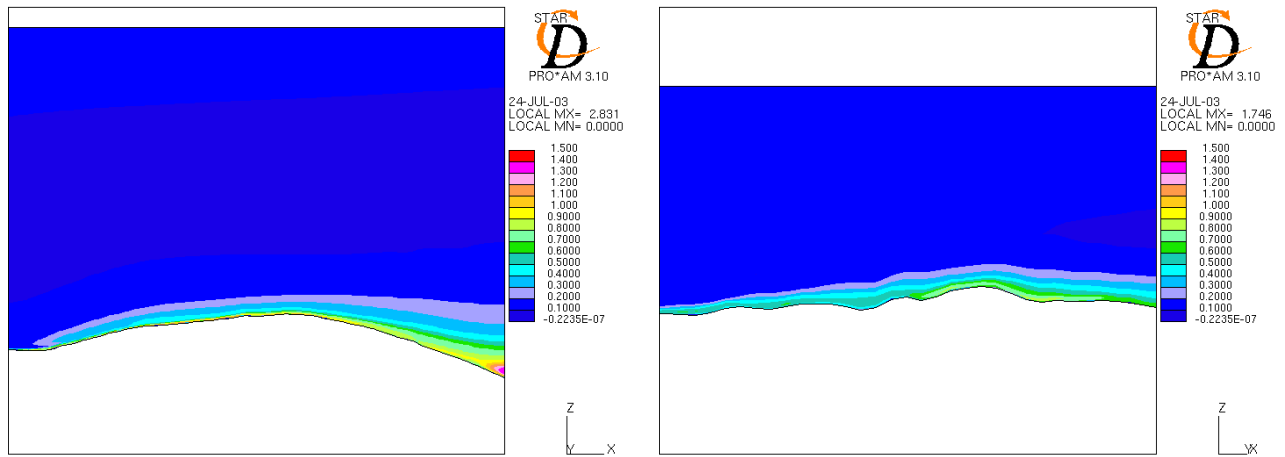
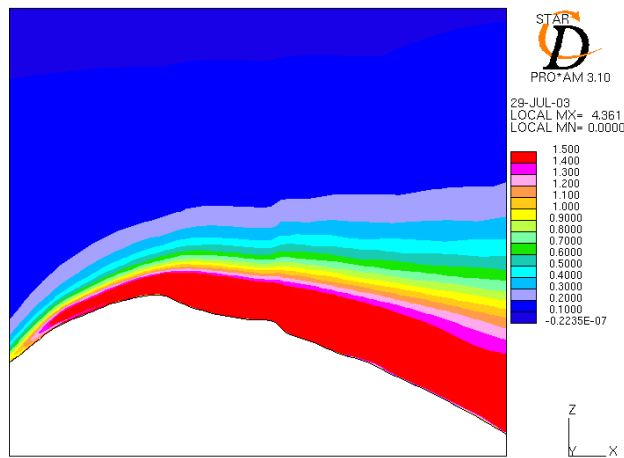


Figure 7. Atacama plateau. Turbulent rms velocity contours in horizontal planes at 5000m (left) and 5400m (right). Wind is from W, resolution is 240m.



**Figure 8.** Cerros de Honar. Turbulent rms velocity contours in vertical planes passing through the ridge, aligned with W (left) and SW (right) wind directions. Resolution is 20m and 200m respectively.



**Figure 9.** Chajnantor summit. Turbulent rms velocity contours in a vertical plane passing through the peak, aligned with the wind direction, W. Resolution is 10m.

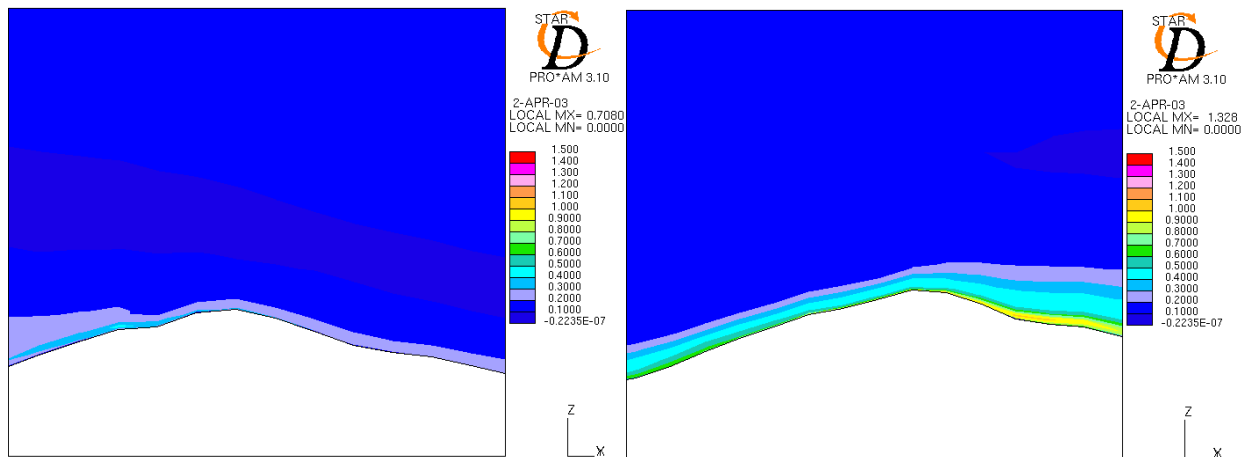


**Figure 10.** Coastal site summit. Turbulent rms velocity contours in a vertical plane passing through the peak, aligned with NE (left) and SW (right) wind directions. Resolution is 200m.